X-Ray Pulsars in a Wide Luminosity Range

A. Mushtukov[1,2,3], V. Suleimanov[4,5], S. Tsygankov[3], D. Nagirner[6], A. Lutovinov[7,8], J. Poutanen[3,9]

E-mail: *al.mushtukov@gmail.com*

A picture of X-ray pulsars (XRPs) behavior in a wide luminosity range is presented. The characteristic accretion luminosity values are discussed as well as connection between XRPs and ultraluminous X-ray sources (ULXs).

1 X-ray pulsars

XRPs stand out from the other classes of accreting NSs due to their strong magnetic field ($\gtrsim 10^{12}$ G), which affects both the geometry of the accretion flow in the vicinity of NS and elementary processes of interaction between radiation and matter.

Magnetic field interrupts the accretion disc (or stellar wind) at the magnetospheric radius, where the magnetic and plasma stresses balance. The magnetospheric radius is given by

$$R_{\rm m} = k \left(\frac{\mu^4}{GM\dot{M}^2} \right)^{1/7},$$

where M and μ are the NS mass and magnetic moment, respectively, $\dot{M}$ is the mass accretion rate and $k \leq 1$ is a constant which depends on the accretion flow geometry ($k = 1$ for the case of spherical accretion and $k < 1$ for the case of accretion from the disc, see [1]). Inside the magnetospheric radius, the magnetic field channels the gas towards the magnetic poles, where the captured matter releases its gravitational energy as X-ray radiation. Some questions concerns the interaction of the accretion flow (stellar wind or accretion disc) and NS magnetosphere [2]. They are important for a self-consistent picture, but beyond the scope of this text.

1 Anton Pannekoek Institute, University of Amsterdam, The Netherlands
2 Pulkovo Observatory of the Russian Academy of Sciences, St. Petersburg, Russia
3 Tuorla Observatory, Department of Physics and Astronomy, Univ. of Turku, Finland
4 Institut für Astronomie und Astrophysik, Universität Tübingen, Germany
5 Kazan (Volga region) Federal University, Russia
6 Sobolev Astronomical Institute, St. Petersburg State University, Russia
7 Space Research Institute of the Russian Academy of Sciences, Moscow, Russia
8 Moscow Institute of Physics and Technology, Russia
9 Nordita, KTH Royal Institute of Technology and Stockholm University, Sweden

V. Grinin et al. (eds) Radiation mechanisms of astrophysical objects. Yerevan: Edit Print, 2017, pp. 339–344.

High magnetic field modifies the elementary processes of interaction between radiation and matter including Compton scattering [3], which defines the radiation pressure and affects spectrum of emergent radiation. In the case of strong magnetic fields, the scattering has a number of special features. Its cross-section can be much smaller than the Thompson scattering cross-section $\sigma_{\rm T}$ depending on magnetic field strength, photon momentum and polarization state. At the same time electron transition between Landau levels causes the resonant scattering at some photon energies, where the cross-section can exceed $\sigma_{\rm T}$ by several orders of magnitude [4, 5]. The resonant scattering leads to appearance of absorption features in the spectra of XRPs – cyclotron lines – and affects the radiation pressure.

2 Below and above the critical luminosity

The accretion luminosity of XRPs is observed to be close or even higher than the Eddington limit $L_{\rm Edd}$ [6], which is commonly used as a restriction of possible isotropic luminosity of the object with a given mass M

$$L_{\rm Edd} = \frac{4\pi G M m_{\rm H} c}{\sigma_{\rm T}(1+X)} \approx 1.4\times 10^{38}\,\frac{M}{M_{\odot}}\,{\rm erg\,s^{-1}}, \tag{1}$$

where $m_{\rm H}$ is the hydrogen mass and X is its mass fraction.

The theory of accretion onto magnetized NS is based on two important effects: the accretion flow is channeled by strong magnetic field, which makes the problem essentially non-spherically symmetrical, and the effective cross-section $\sigma_{\rm eff}$ of the interaction between radiation and matter can be much different from the cross-section in the non-magnetic case.

At low mass accretion rates ($< 10^{16}\,{\rm g\,s^{-1}}$) radiation pressure has only a minor effect on the infalling material. The accretion flow heats up the NS surface and the observed spectrum is shaped by plasma deceleration in the NS atmosphere and by interaction of already emitted radiation with the accretion flow.

The higher the mass accretion rate, the higher the radiation pressure. If the radiation pressure is high enough, it affects the accretion flow velocity. The changes of the accretion flow velocity can be detected from variations of cyclotron line position in the spectrum: the line forms due to the resonant scattering in the accretion flow and, as a result, it is affected by Doppler shifting in the accretion channel [7].

At sufficiently high mass accretion rate the matter is fully stopped by the radiation pressure above stellar surface and an accretion column begins to grow. The corresponding luminosity, which is called critical luminosity, can be estimated as follows [8, 9]:

$$L^{*} = 4\times 10^{36}\,\frac{M/M_{\odot}}{R/10^{6}{\rm cm}}\left(\frac{l_0}{2\times 10^{5}{\rm cm}}\right)\frac{\sigma_{\rm T}}{\sigma_{\rm eff}}\,{\rm erg\,s^{-1}}, \tag{2}$$

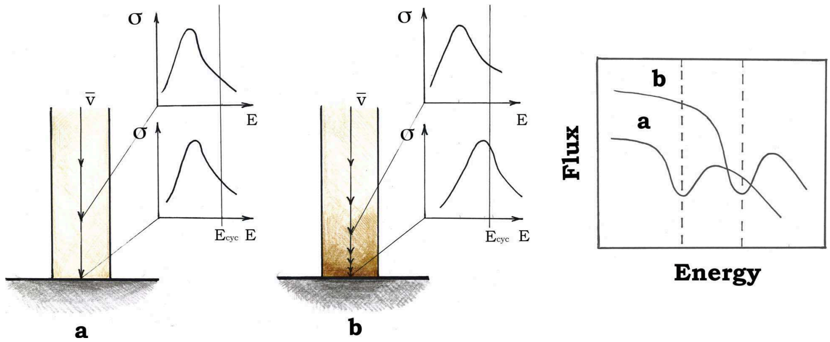

Figure 1: The schematic presentation of the dependence of the cyclotron line energy on the velocity profile in the line-forming region for the case of sub-critical XRPs (see [7] for details).

where R is the NS radius, l_0 is the length of the accretion channel cross-section on the NS surface and $\sigma_{\rm eff}$ is the effective scattering cross-section in strong magnetic field. The value of L^* depends on the surface magnetic field strength due to the strong dependence of the scattering cross-section on the field strength. The critical luminosity is not a monotonic function of B and has its minimum value of $\sim(3\div5)\times10^{36}\,{\rm erg\,s^{-1}}$ at B-field strength of $\sim10^{12}$ G, when the peak in the source spectrum is close to $E_{\rm cycl}$ and the effective radiation pressure reaches its maximum value [9]. For higher magnetic field strength, the critical luminosity value increases due to decrease of the effective scattering cross-section (see Fig. 1).

At the accretion luminosity $L > L^*$ for a given magnetic field strength the accretion flow stops at the radiation dominated shock above the NS surface and slowly settles in inside a sinking region. The luminosity of highly magnetized NS featuring an accretion column above its surface can be much higher than the Eddington luminosity value, because the radiation pressure is balanced by the strong magnetic pressure (instead of gravity), which supports the column. The luminosity of the NS with an accretion column of height H above its surface can be roughly estimated as follows [10]:

$$L^{**}(H) \approx 38\left(\frac{l_0/d_0}{50}\right)\frac{\sigma_{\rm T}}{\sigma_\perp} f\left(\frac{H}{R}\right)L_{\rm Edd}, \qquad f(x)=\log(1+x)-\frac{x}{1+x}, \tag{3}$$

where d_0 is the thickness of the accretion channel, $\sigma_\perp$ is the effective Compton scattering cross-section across the magnetic field direction. For a column as high as the NS radius, the accretion luminosity becomes $L^{**}(H=R)\approx(2\div3)\times 10^{39}\left(\frac{l_0/d_0}{50}\right)\frac{\sigma_{\rm T}}{\sigma_\perp}\,{\rm erg\,s^{-1}}$.

From the comparison of XRPs spectra variability with the theoretical models, we can conclude that the height of the accretion column increases with the mass accretion rate and, indeed, can be comparable to the NS radius [12].

The height of the accretion column is obviously limited by the magnetosphere's radius ($H < R_{\rm m}$). However, many additional conditions have to be taken

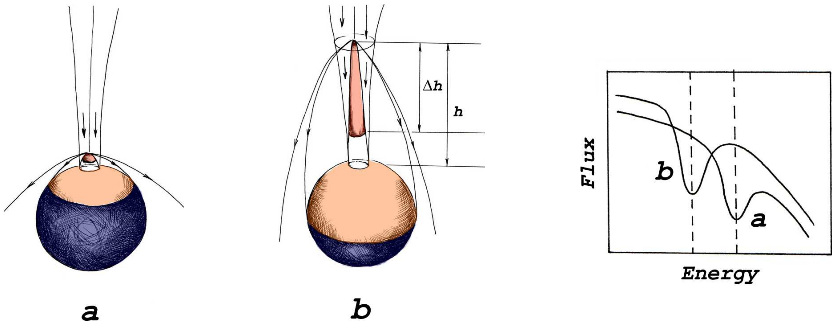

Figure 2: The schematic presentation of the dependence of the cyclotron line energy on the velocity profile in the line-forming region for the case of super-critical XRPs (see [12] for details).

into account. The gas and radiation pressure inside the column should not be higher than the magnetic pressure. This is important for fields of strength below $\sim 2 \times 10^{13}$ G. If the magnetic field strength is higher than $\sim 2 \times 10^{13}$ G, the internal column temperature can reach the value of $\sim 10^{10}$ K, when the electron-positron pair creation with further annihilation into neutrino and anti-neutrino becomes important: $e^{+} + e^{-} \longrightarrow \nu_{\rm e} + \overline{\nu}_{\rm e}$. In this case part of accretion luminosity can be released by neutrino rather than by photons. However, it was shown that the accretion columns above NS with surface B-field strength $\gtrsim 5 \times 10^{13}$ G cannot be significantly higher than NS radius and their internal temperature does not reach values of $\sim 10^{10}$ K [10].

The accretion column structure determines the beam pattern of XRPs [14]. The height of the accretion column, where the matter is stopped by the radiation dominated shock, is different inside the accretion channel. It is caused by the fact that the radiation energy density drops towards the accretion channel edges. As a result, the height reaches its maximum value in the center of the channel and it decreases towards the edges. Therefore, the radiation from the already stopped matter has to penetrate through the layer of fast moving plasma. It leads to the radiation beaming towards the NS surface, where the radiation is intercepted and reprocessed. Changes of the accretion column height and corresponding variability of the illuminated region on the NS surface explain naturally variations of the cyclotron line centroid energy [11] with the accretion luminosity: the higher the mass accretion rate, the higher the column, the lower the magnetic field strength averaged over the illuminated part of the NS, the lower the observed cyclotron line centroid energy [12, 13].

3 XRPs and ULXs

ULXs are point-like extragalactic X-ray sources with an observed X-ray luminosity in excess of $L \sim 10^{39}\,{\rm erg\,s^{-1}}$, assuming that they radiate isotropically. The bolometric luminosity of ULXs exceeds the Eddington limit for accretion on

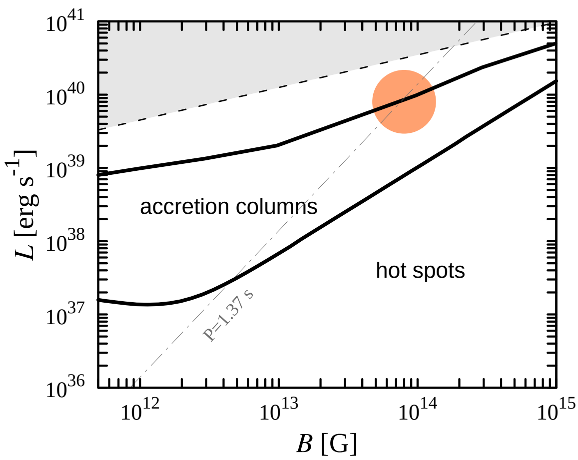

Figure 3: The critical L^* and maximum accretion luminosity values as functions of the B-field strength are given by thick solid lines. The grey region corresponds to the conditions when the accretion disc becomes super-critical. The lower limit on the X-ray luminosity for the case of NS spin period $P = 1.37\,\mathrm{s}$ is shown by dashed-dotted line. It is related to the inhibition of accretion by the propeller effect. The position of the ULX X-2 in galaxy M82 is given by the orange circle.

a $10M_\odot$ black hole (BH). This is, indeed, intriguing since ULXs may be a possible manifestation of sub-critical accretion onto intermediate-mass (masses in the range $\sim 10^2 \div 10^5 M_\odot$) BHs.

At the present time their true nature is not well understood and in fact there may be several types of objects in this category. Most of the models are focused on accretion onto intermediate or stellar mass BHs.

However, it was found by the *NuSTAR* observatory that the ULX X-2 in galaxy M82 shows coherent pulsations with an average period of 1.37 s, which means that the compact object in this particular case is not a BH but a NS [15]. This discovery implies that accreting NS can reach luminosities of about $10^{40}\,\mathrm{erg\,s^{-1}}$ (see Fig. 3), which is two orders of magnitude higher than the Eddington limit. Such high mass accretion luminosity can be explained by extremely high NS magnetic field $\sim 10^{14}\,\mathrm{G}$, which reduces the scattering cross-section and confines the accretion flow to accretion column [10].

It is already confirmed that in this particular case we see accretion onto NS with magnetar-like magnetic field $\sim 10^{14}\,\mathrm{G}$ [16]. According to simple estimations, an accreting NS at such high mass accretion rate reaches the spin equilibrium (when the corotation and magnetosphere radii are equal) within a few hundreds years. As a result, small changes in the mass accretion rate lead to dramatic changes of the accretion luminosity due to the so-called "propeller"-effect, which has been observed in a few XRPs [17]. The mass accretion rate, at which the "propeller"-effect appears, depends on the B-field strength, and the latter can be estimated from the known mass accretion rate. The "propeller"-effect has been observed in ULX M82 X-2 and magnetic field $\sim 10^{14}\,\mathrm{G}$ has been confirmed [16].

The discovery of NSs as compact objects in ULXs puts an additional important question: what fraction of ULXs are accreting NSs? It is interesting that no other pulsating ULX has been observed yet. According to our recent results, the accretion luminosity of a few$\times 10^{40}$ erg s^{-1} is a good estimation for maximum NS accretion luminosity [10]. This luminosity coincides with the cut-off observed in the HMXBs luminosity function (ULXs are taken into account there as HMXB) which otherwise does not show any features at lower luminosities [18]. Therefore one can conclude that a substantial fraction of ULXs are accreting NSs.

References

1. *J. Frank, A. King, D. Raine*, Accretion Power in Astrophysics. Cambridge: Cambridge Univ. Press, 2002.
2. *D. Lai*, Phys. J. Web Conf., **64**, 1001, 2014.
3. *A.K. Harding, D. Lai*, Rep. Prog. Phys., **69**, 2631, 2006.
4. *A.A. Mushtukov, D.I. Nagirner, J. Poutanen*, Phys. Rev. D, **85**, 103002, 2012.
5. *A.A. Mushtukov, D.I. Nagirner, J. Poutanen*, Phys. Rev. D, **93**, 105003, 2016.
6. *R. Walter, A.A. Lutovinov, E. Bozzo, S.S. Tsygankov*, Astron. Astrophys. Rev., **23**, 2, 2015.
7. *A.A. Mushtukov, S.S. Tsygankov, A.V. Serber et al.*, Mon. Not. Roy. Astron. Soc., **454**, 2714, 2015.
8. *M.M. Basko, R.A. Sunyaev*, Mon. Not. Roy. Astron. Soc., **175**, 395, 1976.
9. *A.A. Mushtukov, V.F. Suleimanov, Sergey S. Tsygankov, J. Poutanen*, Mon. Not. Roy. Astron. Soc., **447**, 1847, 2015.
10. *A.A. Mushtukov, V.F. Suleimanov, S.S. Tsygankov, J. Poutanen*, Mon. Not. Roy. Astron. Soc., **454**, 2539, 2015.
11. *S.S. Tsygankov, A.A. Lutovinov, E.M. Churazov, R.A. Sunyaev*, Mon. Not. Roy. Astron. Soc., **371**, 19, 2006.
12. *J. Poutanen, A.A. Mushtukov, V.F. Suleimanov et al.*, Astrophys. J., **777**, 115, 2013.
13. *A.A. Mushtukov, J. Poutanen, V.F. Suleimanov et al.*, Phys. J. Web Conf., **64**, 2005, 2014.
14. *A.A. Lutovinov, S.S. Tsygankov, V.F. Suleimanov et al.*, Mon. Not. Roy. Astron. Soc., **448**, 2175, 2015.
15. *M. Bachetti, F.A. Harrison, D.J. Walton et al.*, Nature, **514**, 202, 2014.
16. *S.S. Tsygankov, A.A. Mushtukov, V.F. Suleimanov, J. Poutanen*, Mon. Not. Roy. Astron. Soc., **457**, 1101, 2016.
17. *S.S. Tsygankov, A.A. Lutovinov, V. Doroshenko et al.*, Astron. Astrophys., **593**, A16, 2016.
18. *S. Mineo, M. Gilfanov, R. Sunyaev*, Mon. Not. Roy. Astron. Soc., **419**, 2095, 2012.

* The color figures are available online in the Proceedings at *http://www.astro.spbu.ru/sobolev100/*.